J Geod (2012) 86:681–694
DOI 10.1007/s00190-012-0547-6

ORIGINAL ARTICLE

The Gauss–Listing geopotential value W_0 and its rate from altimetric mean sea level and GRACE

N. Dayoub · S. J. Edwards · P. Moore

Received: 16 March 2011 / Accepted: 13 February 2012 / Published online: 10 March 2012
© Springer-Verlag 2012

Abstract In geopotential space, the fundamental geodetic parameter W_0 defines the Gauss–Listing geoid which can be used to best represent the Earth's mean sea level (MSL) and hence specifies a conventional zero height level to unify vertical datums employed by mapping agencies throughout the world. Further, W_0 cannot be considered invariant as the parameter varies temporally as a direct response to sea level change and mass redistributions. This study determines W_0 and its rate, $\mathrm{d}W_0/\mathrm{d}t$, by utilizing altimetric MSL models and an independent mean dynamic topography (MDT) model to define points on the geoid. W_0 and $\mathrm{d}W_0/\mathrm{d}t$ are estimated by two approaches: (i) by means of a global gravity field model (GGM) and (ii) within normal gravity field space as the geopotential value of the best fitting reference ellipsoid. The study shows that uncertainty in W_0 is mainly influenced by MDT while the choice of methodology, GGM and MSL data coverage are not significant within reason. Our estimate $W_0 = 62636854.2 \pm 0.2\ \mathrm{m}^2\,\mathrm{s}^{-2}$ at epoch 2005.0 differs by $1.8\,\mathrm{m}^2\mathrm{s}^{-2}$ from the International Astronomical Union reference value. This study shows that, at a sub-decadal time scale, the time variation $\mathrm{d}W_0/\mathrm{d}t$ stems mainly from sea level change with negligible effect from gravity field variations. $\mathrm{d}W_0/\mathrm{d}t = (-2.70 \pm 0.03) \times 10^{-2}\,\mathrm{m}^2\,\mathrm{s}^{-2}\,\mathrm{year}^{-1}$, corresponding to a MSL rise of 2.9 mm year^{-1}, is evaluated from sea level change based on 16 years of TOPEX and Jason-1 data.

Keywords Gauss–Listing geoid · Geopotential · GRACE: Satellite Altimetry · Variation of W_0 with time · W_0

1 Introduction

Progress towards the precise definition and realization of a unified global vertical datum has been advanced by recent developments in GNSS, satellite altimetry, surface gravimetry and geodetic techniques and processing strategies. In geopotential space, this involves adoption of a global potential value to define the zero height datum (Sanchez 2007, 2009). An intuitive value is the fundamental geodetic parameter, W_0, that classically defines the Gauss–Listing geoid as the best fitting equipotential surface to mean sea level (MSL). The vertical coordinates of the local datum used by the mapping agency are given unambiguously by geopotential numbers referred to W_0. Any other point in a local datum can be defined similarly in the global vertical system. The conversion from geopotential number to height is then one of realization. A difficulty with the above definition is that the Gauss–Listing geoid as an equipotential surface departs from MSL due to non-gravitational effects with the deviation called either sea surface topography (SST) or mean dynamic topography (MDT). Furthermore, with recent advances in space geodetic techniques and gravity field measurement, the geoid cannot be considered as a static surface as sea level change and mass redistribution affect the geoid surface with associated time variation in W_0.

Several studies have estimated W_0 using a variety of techniques and datasets. In particular, a series of papers by Burša and colleagues (Burša et al. 1997, 1998, 1999a,b, 2001, 2004, 2007a,b) investigated the global determination of W_0 using data from satellite altimetry over the oceans. They concluded that W_0 is independent of the tidal reference system of the

N. Dayoub · S. J. Edwards · P. Moore
School of Civil Engineering and Geosciences,
Newcastle University, Newcastle NE1 7RU, UK

Present Address:
N. Dayoub (✉)
Department of Topography, Faculty of Civil Engineering,
Tishreen University, P.O. BOX 2230, Lattakia, Syria
e-mail: Nadim.Dayoub@Tishreen.edu.sy

gravity field and relatively insensitive to degree $n > 120$ of the global gravity field (GGM) model. Their value $W_0 = 62636856.0 \pm 0.5\ \mathrm{m^2\,s^{-2}}$ is the numerical value included in the International Astronomical Union report on astronomical constants (Luzum et al. 2011). In a comparable study, Sanchez (2007) determined W_0 from different GGMs, namely EGM96 (Lemoine et al. 1998), TEG4 (Tapley et al. 2001), GGM02S (Tapley et al. 2005) and EIGEN-CG03C (Förste et al. 2005). Sanchez (2007) revealed that the choice of geopotential model is unimportant but that the latitude domains of the altimetric MSL are significant. On using EIGEN-CG03C to degree $n = 360$ for data between $60°/60°$ Sanchez (2007) gave $W_0 = 62636853.4\ \mathrm{m^2\,s^{-2}}$. This differs by $2.6\ \mathrm{m^2\,s^{-2}}$ from the IAU reference value. As an alternative to the global approach, Ardalan et al. (2002) estimated W_0 by utilizing the ellipsoidal harmonic expansion of EGM96 to degree/order 360/360 using data from tide gauges and nearby GPS sites around the Baltic Sea.

Secular variation in W_0 has been estimated from sea level change on a regional basis using tide gauge and GPS observations (Ardalan et al. 2002) and globally using sea level time series from radar altimetry (Burša et al. 1999a, 2007a). These studies essentially used static gravity fields. However, the harmonic coefficients have signatures of a periodic, quasi-secular and secular nature (Moore et al. 2006). This suggests that determination of $\mathrm{d}W_0/\mathrm{d}t$ should consider the potential effect of a dynamic gravity field. Accordingly, we utilize monthly gravity field solutions from the Gravity Recovery and Climate Change Experiment (GRACE) (Tapley et al. 2004). As GRACE gives anomalous values for the degree two zonal harmonic, C_{20} (Chambers 2006; Chen et al. 2005), we replace these values with those from satellite laser ranging (SLR) (Cheng and Tapley 2004). C_{20} is critical to mass variations, with the secular change in the Earth's oblateness reported as $1.23 \times 10^{-11}\ \mathrm{year^{-1}}$ based on 28 years of SLR data (Cheng and Tapley 2004). Consideration is also given to the degree one harmonics associated with geocentre variations which could have an effect on ocean mass trends of a few tenths of $\mathrm{mm\,year^{-1}}$ (Swenson et al. 2008).

The aim of this study is twofold. Firstly, we aim to resolve the uncertainty in the published values of W_0 by re-examination of the methodologies and datasets underpinning the global approach. We consider two methodologies; namely estimation of W_0 using GGMs and the normal gravity field. Both approaches use data from altimetry-based global MSLs and an MDT model. In particular, W_0 is estimated by evaluating the GGM to a certain degree/order over the ocean to obtain the mean W_0 using an equal-area weighting function. The analysis identifies sensitivity of the analysis to the underlying parameterisation including the Earth's gravitational field model (resolution, and choice of model), the data coverage and MDT. Alternatively, W_0 is estimated through the normal gravity field as the geopotential value of the best-fitting ellipsoid to the geoid. The roles of data coverage and MDT are again investigated. Secondly, we investigate the determination of $\mathrm{d}W_0/\mathrm{d}t$. Sea level change is estimated by utilizing data between $66°\mathrm{N}/66°\mathrm{S}$ using TOPEX and JASON-1 sea surface heights (1992.9–2009.0), while variations in the Earth gravity field are inferred from GRACE and SLR measurements. Alternatively, $\mathrm{d}W_0/\mathrm{d}t$ is estimated indirectly within the normal gravity field by estimating the secular changes in the semi-major and semi-minor axes of the best fitting ellipsoid to the geoid.

2 W_0: Determination methodology

The geopotential value at a point P is given by Torge (1967, pp 20 and pp 28)

$$W(\phi,\lambda,r) = \frac{\mathrm{GM}}{a_\mathrm{E}} \sum_{n=0}^{\infty} \sum_{m=0}^{n} \left(\frac{a_\mathrm{E}}{r}\right)^{(n+1)} P_{nm}(\sin\phi) \times (C_{nm}\cos m\lambda + S_{nm}\sin m\lambda) + \frac{1}{2}\omega^2 r^2 \cos^2\phi \tag{1}$$

where ϕ, λ, r are the spherical latitude, longitude and radial distance of P, respectively, GM the product of the gravitational constant and the Earth's mass, a_E the reference semi-major axis of the Earth's ellipsoid, ω the Earth's angular velocity, C_{nm} and S_{nm} the fully normalized harmonic coefficients of degree n and order m and $P_{nm}(\sin\phi)$ the fully normalized associated Legendre functions of the first kind. The degree one coefficients in Eq. (1) are taken to be zero as the origin of the coordinate system coincides with the centre of mass of the Earth.

In Fig. 1, $E(a_0, b_0)$ is the best-fitting ellipsoid to the geoid defined by semi-major axis, a_0, semi-minor axis, b_0, ω and GM_0; N is the geoid height. The normal potential value, U_0, on the surface of this ellipsoid is given by Heiskanen and Moritz (1967, pp 67)

$$U_0 = \frac{\mathrm{GM}_0}{\varepsilon} \tan^{-1}\left(\frac{\varepsilon}{b_0}\right) + \frac{1}{3}\omega^2 a_0^2, \tag{2}$$

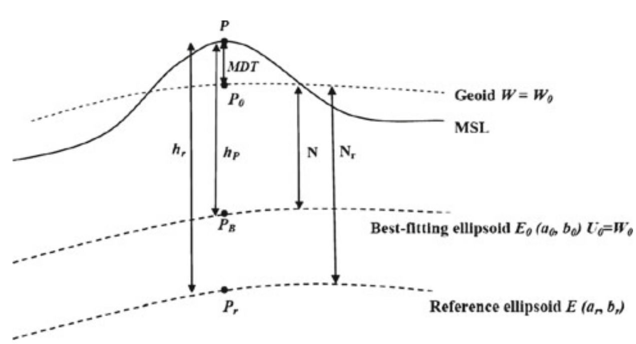

Fig. 1 Geoid, ellipsoids and W_0

where ε is the linear eccentricity, $\varepsilon^2 = a_0^2 - b_0^2$.

Utilizing the above equations the fundamental parameter W_0 can be determined by consideration of:

(i) points on the geoid and a gravitational field model using Eq. (1), or
(ii) the parameters a_0 and b_0 of the best fitting ellipsoid using Eq. (2).

2.1 GGM and MSL

Within the method (i) datasets of sea-level heights from altimetry-based MSLs are used together with a MDT model to establish geodetic coordinates of the geoid. As MSL is by definition averaged over the time span of the data underpinning the model, it is to be expected that mean sea-level heights will vary from one model to another depending on the data sets employed in the derivations. To establish the geodetic height relative to the reference ellipsoid, we use

$$N_r(\phi, \lambda) = h_r(\phi, \lambda) - \mathrm{MDT}(\phi, \lambda) \tag{3}$$

where h_r is the ellipsoidal height of a point on MSL (Fig. 1). Initially, to investigate its significance, MDT is ignored in Eq. (3). Three GGMs were used to degree/order 360/360, namely EGM96, EGM2008 (Pavlis et al. 2008) and EIGENGL04C (Förste et al. 2008). As W_0 is independent of the permanent tide (Burša et al. 1999b), we use the mean tide system for convenience. We use MSLs derived from TOPEX and Jason-1 as well as the mean sea-surface models MSSCLS01 (for brevity CLS01) (Hernandez and Schaeffer 2001) and DNSC08 (Andersen and Knudsen 2009) to quantify the dependence of W_0 on the MSL model and to facilitate comparison with other published values.

2.1.1 *W_0: MSL from CLS01 and DNSC08*

CLS01 was constructed using altimetry from GEOSAT (1987–1988), ERS-1/2 (1993–1999), TOPEX/Poseidon (1993–1999) and the geodetic phase of ERS-1 (1994–1995). Model values are supplied on a continuous surface between geodetic latitudes 82°N and 80°S including heights from the EGM96 geoid over land with a cosine tapering performed to smooth the connection between the altimetry and land values. The more recent DNSC08 model was based on radar altimetry (GEOSAT 1985–1986, TOPEX/Poseidon 1993–2004, ERS-1/2 1994–2003.5, GEOSAT follow on (GFO) 2000–2004, ENVISAT 2003–2004) and laser altimetry from ICESat (2005–2006). Since ICESat data were used in the ice-covered part of the Arctic Ocean (72° − 86°) which is beyond the range of the MDT model of this study, we can assign a median date of 1998.5 to DNSC08. Similarly, for CLS01, we assign a date of 1996.0, namely the median of the TOPEX/Poseidon data.

The gravity potential values from EGM96, EGM2008 and EIGENGL04C to degree and order 360 were estimated at each point of a 0.5° × 0.5° grid of CLS01 and then averaged globally using an equal area weighting function. The GGMs were referenced to mean epoch 1996.0, although for later use EGM2008 is evaluated at epoch 2005.0. Results in Table 1, derived without correction for MDT, show that the choice of GGM has no significant effect on W_0. Additional tests showed that a higher resolution grid for the MSL has negligible effect on the values with the changes being less than the standard deviations in Table 1. In agreement with Sanchez (2007), data coverage has the largest influence causing W_0 to vary by 1 $\mathrm{m^2\,s^{-2}}$ as the domain is reduced from 82°N/80°S to 60°N/60°S. Our estimated W_0 from CLS01 for 60°N/60°S is in excellent agreement (see also Table 7) with Sanchez (2007) but departs from Burša et al. (2007a). For comparison, Table 1 presents DNSC08 values at epoch 2005.0. It is noted that W_0 is higher with DNSC08. There are a number of possibilities to explain this including the time span of data used to construct the MSL models and enhancements to altimetric processing and corrections. This aspect will be investigated below.

To establish the spectral resolution of the GGM, W_0 has been determined with respect to CLS01 using the aforementioned GGMs for degrees between 6 and 360. Figure 2 confirms that for all GGMs, high degree harmonics do not influence the global estimation. It should be stated that, in

Table 1 W_0 derived from the CLS01 (DNSC08) model (without correction for MDT) and GGMs to degree/order 360/360 in the mean tide system at different latitude domains

	$W_0 - 62636850$ ($\mathrm{m^2s^{-2}}$)				ϕ N/S
	EGM96 1996.0	EIGEN-GL04C 1996.0	EGM2008 1996.0	EGM2008 2005.0	
CLS01	4.49 ± 0.03	4.47 ± 0.03	4.46 ± 0.03	4.22 ± 0.03	82°/80°
CLS01	4.30 ± 0.03	4.27 ± 0.03	4.25 ± 0.03	4.01 ± 0.03	70°/70°
CLS01	3.48 ± 0.03	3.44 ± 0.03	3.43 ± 0.03	3.19 ± 0.03	60°/60°
DNSC08				4.43 ± 0.03	82°/80°
DNSC08				4.24 ± 0.03	70°/70°
DNSC08				3.43 ± 0.03	60°/60°

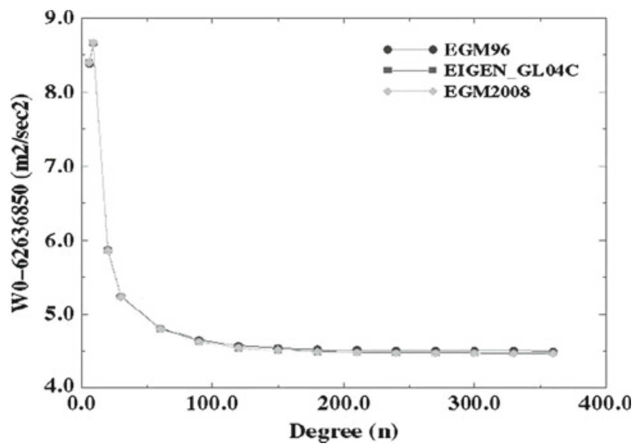

Fig. 2 Dependence of W_0 on degree n of GGM using data from the CLS01 model for latitude band 82°N–80°S

general, it is inadvisable to truncate a gravity model such as EGM2008 but the insensitivity to higher degree harmonics suggests that truncation has negligible impact. The insensitivity of the geopotential to the higher degree harmonics and the sufficiency of a relatively coarse grid for this analysis are consequences of the relative smoothness of Eq. (1) as a function of latitude and longitude.

To investigate the effect of MDT on W_0 and on the latitudinal dependence of W_0 in Table 1 the Estimating the Circulation and Climate of the Ocean, phase II (ECCO-2) model (Menemenlis et al. 2008) was used. ECCO-2 is jointly constructed by JPL, the Massachusetts Institute of Technology (MIT) and the Scripps Institution of Oceanography. The ECCO-2 MDT covers latitudes 78°N to 78°S. To utilize the MDT heights, it is noted that surfaces of constant height in ocean models are also equipotential surfaces (Hughes and Bingham 2008) while the ocean model latitude should be interpreted as geodetic. ECCO-2 uses observed sea-level anomalies from altimetry with a GRACE-based MDT (Rio et al. 2005) as observational constraints. However, it is not clear that the zero level refers to the geoid of date and hence differences may appear in W_0 computed with alternative MDT models. The important factor here is that the ECCO-2 MDT is not computed directly as the difference between an altimetric sea surface and a geoid model but as an ocean state within a global circulation model. In ECCO-2, MDT is supplied as a single default value for latitude 72.5°–78° N/S which limits the use of the full CLS01/DNSC08 models to say 70°/70° N/S. The MDT-adjusted geoid heights were estimated from Eq. 3. Only EGM2008 to degree/order 360/360 was used. Table 2 shows that MDT has a significant effect on W_0 eliminating the dependency of W_0 on the latitude domain for both CLS01 and DNSC08. Use of MDT has also reduced the standard deviations by a factor of three. However, W_0 with DNSC08 is still larger than with CLS01 despite our efforts at removing the MDT which suggests that

Table 2 W_0 with 95% confidence limits derived from CLS01 (referenced to 1996.0), DNSC08 (referenced to 1998.5) and EGM2008 to degree/order 360/360 in the mean tide system. MDT from ECCO-2 at different latitude domains

MSL	$W_0 - 62636850$ ($\mathrm{m^2s^{-2}}$)		ϕ N/S
	1996.0/1998.5	2005.0	
CLS01	4.29 ± 0.01	4.05 ± 0.01	70°/70°
	4.25 ± 0.01	4.01 ± 0.01	60°/60°
DNSC08	4.44 ± 0.01	4.26 ± 0.01	70°/70°
	4.38 ± 0.01	4.20 ± 0.01	60°/60°

more recent enhancements in altimetric processing are the most likely cause.

2.1.2 W_0: MSL from TOPEX/Poseidon and Jason-1

To further investigate any dependence of W_0 on the altimetric data itself, and for later use in $\mathrm{d}W_0/\mathrm{d}t$ estimation, sea surface heights from TOPEX/Poseidon (T/P) and Jason-1 (J1) have been used to establish MSLs. For T/P, we used cycles 9–364 (December 1992–August 2002) from the Merged Geophysical Data Record (GDR-M) version C; Poseidon data were discarded. For J1, we used release C of the Geophysical Data Records (GDR) for cycles 1–258 (January 2002–January 2009). Beckley et al. (2007) examined the effect of the orbits computed with ITRF2005 and an updated gravity field on the altimetric sea level trends compared with earlier releases and reported an accelerated sea level rise compared with earlier solutions. It is noted that J1 release C is the latest version available with orbits computed using ITRF2005 and the GRACE gravity field EIGEN-GL04S (Förste et al. 2008) although the T/P version C is based on the JGM3 (Tapley et al. 1996) gravity field from the pre-GRACE era. However, we show later (Fig. 7) that there is not a significant difference in trend by combining T/P and J1 altimetry.

We applied the corrections for the dry tropospheric effect, the ionospheric effect, the geocentric ocean tide, the solid Earth tide and the pole tides as given on the GDR. For T/P, the wet troposphere correction was modified from Keihm et al. (1998) for the drift in one channel of the TOPEX microwave radiometer (TMR) (Keihm et al. 2000). Also applied were the TMR yaw correction (Zlotnicki and Callahan 2002) and the T/P correction coefficients for the sea state bias (Chambers et al. 2003). However, the inverse barometer (IB) correction provided by GDR-M is based on the variation of the atmospheric pressure from a constant value (i.e., 1,013.3 mbar) which is not appropriate for our study. This was replaced for T/P by the mean global pressure over the ocean per cycle (Dorandeu and Le Traon 1999).

For both satellites, coastal (e.g., TMR flagged over land) and shallow seas (<1,000 m depth) and sea-ice were

Table 3 W_0 in the mean tide system: TOPEX MSL and EGM2008 to degree/order 360/360 with and without MDT from ECCO-2 at different latitude domains

Cycles	N/S	$W_0 - 62636850$ ($m^2\,s^{-2}$)		MDT
		1997.8	2005.0	
T/P 9–364	66°/66°	3.69 ± 0.02	3.50 ± 0.02	–
	60°/60°	3.50 ± 0.02	3.31 ± 0.02	–
	66°/66°	4.39 ± 0.01	4.20 ± 0.01	ECCO-2
	60°/60°	4.38 ± 0.01	4.19 ± 0.01	ECCO-2

Table 4 W_0 in the mean tide system: Jason-1 MSL and EGM2008 to degree/order 360/360 with and without MDT from ECCO-2 at different latitude domains

Cycles	N/S	$W_0 - 62636850$ ($m^2 s^{-2}$)		MDT
		2005.52	2005.0	
J1 1–258	66°/66°	3.48 ± 0.02	3.49 ± 0.02	–
	60°/60°	3.26 ± 0.02	3.27 ± 0.02	–
	66°/66°	4.16 ± 0.01	4.17 ± 0.01	ECCO-2
	60°/60°	4.16 ± 0.01	4.17 ± 0.01	ECCO-2

excluded as data quality is expected to be poor. In addition, only points measured in at least 75% of the total cycles were included to avoid variance in the number of ocean data points, especially near the South Pole due to seasonal sea-ice. The corrected sea surface heights were interpolated to standard latitudinal points with spacing equivalent to a 10 s displacement along track. To determine MSL at the standard points, we solved for corrections at tidal constituents O1, K1, N2, M2, S2, K2 and SA corresponding to signatures at 45.714, 173.193, 49.528, 62.108, 58.742, 86.596 and 365.25 days, respectively (Schlax and Chelton 1996). The T/P MSL is referenced to 1997.8 and that from J1 to 2005.52. Two latitude domains were used, namely 66°/66° and 60°/60° N/S with W_0 estimated with and without MDT from ECCO-2. Results from T/P and J1 are presented in Tables 3 and 4.

It is important to note that the absolute altimetric range bias for the TOPEX/Poseidon MSL is statistically indistinguishable from zero at the 15 mm level (Haines et al. 2010) whilst Jason-1 shows a bias of 94 ± 15 mm. Accordingly, the T/P MSL can be used as an unbiased measure of the sea surface to which Jason-1 can be adjusted during the tandem mission with T/P. During the first 20 repeat cycles (i.e., 200 days), the two altimetric satellites were flown in identical tandem orbits about 70 s apart. Thus, during the tandem mission, the altimeters onboard the respective satellites effectively sampled the same ocean variability enabling a precise cross-calibration of the range difference. In this study, the global difference between W_0 for each of the 20 cycles was averaged to yield 1.18 $m^2\,s^{-2}$. This offset was subsequently used to adjust J1 to the equivalence of an unbiased T/P value.

To compare Tables 2, 3 and 4, it is necessary to adopt a common reference epoch to eliminate the influence of sea level change on W_0. We adopt the secular trend $dW_0/dt = -2.70 \times 10^{-2} \pm 0.03 \times 10^{-2}\,m^2\,s^{-2}\,year^{-1}$ (Sect. 3) based on data from TOPEX and Jason-1 between 1992.9 and 2009.0. Comparison of W_0 derived from T/P, J1 and DNSC08 at epoch 2005.0 shows excellent agreement with differences consistent with the given standard deviations. The consistency between the T/P and J1 mean sea surfaces and DNSC08 adds further weight to the argument that improvements in altimetric processing are the cause of the $\approx 0.20\,m^2\,s^{-2}$ difference (equivalent to about 2.0 cm in geoid height) with CLS01.

2.2 W_0: Normal gravity field

In an alternative methodology (Vaníček and Krakiwsky 1982, pp 115; Burša, 1997) that does not use a GGM explicitly, W_0 is determined indirectly as the normal geopotential value, Eq. (2), of the best fitting ellipsoid to the geoid. The problem (see Fig. 1) is equivalent to

$$\min \int_{S_0} \left(h_p(\varphi, \lambda, a_0, b_0) - \mathrm{MDT}(\varphi, \lambda)\right)^2 \mathrm{d}S \tag{4}$$

with respect to a_0, b_0 where $h_p(\varphi, \lambda, a_0, b_0)$ is the ellipsoidal height of point P on the mean sea surface with respect to the best fitting ellipsoid, and S_0 represents the equipotential surface derived by removing MDT from the mean sea surface. In Eq. (4), φ, λ are the reduced geodetic latitude and longitude, respectively, with the infinitesimal surface area $\mathrm{d}S = (b_0^2 + \varepsilon^2 \sin^2 \varphi) \cos\varphi d\varphi d\lambda$ (Heiskanen and Moritz 1967, pp 41).

The disturbing potential at P_0 is $T(P_0) = W(P_0) - U(P_0)$. Using Taylor series at P_0 to expand the function U about point P_B in the direction n gives

$$T(P_0) = W(P_0) - \left[U(P_B) + (h_p - \mathrm{MDT}) \left.\frac{\partial U}{\partial n}\right|_{P_B} \right] \tag{5}$$

As $W(P_0) = W_0$ and $U(P_B) = U_0$ Eq. (5) simplifies to

$$T(P_0) = (h_p - \mathrm{MDT})\gamma(P_B) \tag{6}$$

where we have used $W_0 = U_0$ and $\left.\frac{\partial U}{\partial n}\right|_{P_B} = -\gamma(a_0, b_0, P_B)$; γ denotes the normal gravity acceleration. We can now replace $h_p - \mathrm{MDT}$ in Eq. (4) to give

$$\min \int_{S_0} \left(\frac{T(P_0)}{\gamma(a_0, b_0, P_B)} \right)^2 \mathrm{d}S \tag{7}$$

where

$$T(P_0) \equiv T(a_0, b_0, P_0) = W_0 - U(a_0, b_0, P_0)$$
$$= U_0(a_0, b_0) - U(a_0, b_0, P_0). \quad (8)$$

As shown in Fig. 1, our mean sea-surface heights, h_r, are given with respect to a reference ellipsoid $E(a_r, b_r)$ defined by semi-major axis a_r, and semi-minor axis b_r,. Let $a_0 = a_r + \Delta a$ and $b_0 = b_r + \Delta b$, then Taylor series applied to Eq. (8) yields

$$\begin{aligned} T(a_0, b_0, P_0) &= U_0(a_r, b_r) - U(a_r, b_r, P_0) \\ &\quad - \left(\frac{\partial U}{\partial a} - \frac{\partial U_0}{\partial a}\right)\Delta a - \left(\frac{\partial U}{\partial b} - \frac{\partial U_0}{\partial b}\right)\Delta b \\ &\equiv \Delta U - U_a \Delta a - U_b \Delta b \end{aligned} \quad (9)$$

where all partial derivatives are evaluated on the reference ellipsoid.

In Eq. (7), we can approximate $\gamma(a_0, b_0, P_B)$, namely normal gravity evaluated at the reduced latitude φ on the best fitting ellipsoid, by $\gamma(a_0, b_0, P_B) \approx \gamma(a_r, b_r, P_r)$. This is possible due to the small height differences and the restriction to a first-order approximation. Thus, substituting Eq. (9) into Eq. (7) gives

$$\min \int_{S_0} \left(\frac{\Delta U - U_a \Delta a - U_b \Delta b}{\gamma(a_r, b_r, P_r)}\right)^2 \mathrm{d}S \quad (10)$$

The quantity ΔU in Eq. (10) is given by

$$\begin{aligned} \Delta U &= U_0(a_r, b_r) - U(a_r, b_r, P_0) \\ &= (h_r - \mathrm{MDT})\gamma(a_r, b_r, P_r) \end{aligned} \quad (11)$$

on expanding the second term about P_r in the direction n and using $\frac{\partial U}{\partial n}\big|_{P_r} = -\gamma(a_r, b_r, P_r)$ and the identity $U_0(a_r, b_r) \equiv U(a_r, b_r, P_r)$. The partial derivatives of Eq. (9) can be derived (Burša et al. 1997) by utilizing the potential of normal gravity (Heiskanen and Moritz 1967, pp 67), namely

$$\begin{aligned} U(a, b, P) &= \frac{\mathrm{GM}}{\varepsilon} \tan^{-1}\frac{\varepsilon}{u} + \frac{\omega^2}{2} a^2 \frac{q}{q_0}\left(\sin^2\varphi - \frac{1}{3}\right) \\ &\quad + \frac{\omega^2}{2}(u^2 + \varepsilon^2)\cos^2\varphi \\ q &= \frac{1}{2}\left[\left(1 + 3\frac{u^2}{\varepsilon^2}\right)\tan^{-1}\frac{\varepsilon}{u} - 3\frac{u}{\varepsilon}\right], \quad q_0 = q_{u=b} \end{aligned} \quad (12)$$

In Eq. (12), the point P is expressed in ellipsoidal coordinates (u, φ, λ) where u is the semi-minor axis of an ellipsoid passing through P with a and b the semi-major and semi-minor axes, respectively, of the reference ellipsoid. The semi-major axis, a, is connected to the linear eccentricity ε and b by $a = \sqrt{b^2 + \varepsilon^2}$. In addition, Eq. (9) utilizes

$$U_0(a, b) = \frac{\mathrm{GM}_0}{\varepsilon}\tan^{-1}\left(\frac{\varepsilon}{b}\right) + \frac{1}{3}\omega^2 a^2 \quad (13)$$

Eq. (13) reduces to Eq. (2) on the best fitting ellipsoid.

By approximating Eq. (10) by a summation over lat/lon blocks of a $1° \times 1°$ grid and minimising with respect to Δa and Δb yields changes to the semi-major and semi-minor axes that adjust the reference ellipsoid to the best fitting ellipsoid to the geoid. However, the method needs full global data coverage (Burša et al. 1997). To fill-in areas over land and the coastal zone, we computed the geoid heights from EGM2008 using the method of Lemoine et al. (1998) and Rapp (1997) utilizing the maximum degree and order of EGM2008. The computation of geoid undulations from EGM2008 requires assignment of a value for W_0. For test purposes only, the geoid was assigned a value of $W_0 = 62636854.46\,\mathrm{m}^2\,\mathrm{s}^{-2}$ at 1996.0 obtained from Table 1 for latitude limits 82°N–80°S to match the CLS01 MSL.

In order to derive geoid heights over the continents from EGM2008, the associated digital elevation model, DTM 2006.0, was used in the form of fully normalized spherical harmonic coefficients of the elevation to degree/order 2190/2190 (http://users.auth.gr/~kotsaki/IAG_JWG/IAG_JWG). All EGM2008 geoid heights were transformed into the mean tide system for consistency with CLS01. For the test case, the combined land/ocean surface was examined globally to investigate potential disparities between the CLS01 MSL and the EGM2008 geoid in coastal areas. All checks showed good agreement between the two surfaces in these areas.

All heights were computed relative to the reference T/P ellipsoid defined by $a_r = 6378136.30$ m and $b_r = 6356751.601$ m with $\mathrm{GM}_0 = 398600441.8 \times 10^6\,\mathrm{m}^3\mathrm{s}^{-2}$ and $\omega = 7292115 \times 10^{-11}$ rad s^{-1}. To avoid influencing the solution with the *a priori* value, we iterated with W_0 in the EGM2008 heights, utilizing the latest derived value until W_0 converged. Experiments showed that the results were independent of the *a priori* value with consistency of solution irrespective of the starting value. Table 5 presents results for three different cases: (i) full global data coverage with no MDT applied, (ii) full global data coverage with MDT from ECCO-2 and (iii) data over the ocean with no MDT considered. W_0 for cases (i) and (ii) are identical, although Δa and Δb differ significantly while (iii) gives unrealistic results which confirms the necessity of full global data coverage in this approach. It was noted that the lack of high latitude information in the MSL data leads to a high correlation between a and b that is resolved when the additional data is added. Computations were repeated with CLS01 replaced by DNSC08. The sensitivity of the parameters to the MSL model is low with Δa being near identical although Δ b exhibits differences at the 2–3 cm level. The derived W_0 values are almost insensitive to the MDT with close agreement between CLS01 and DNSC08.

To compare the results from Tables 1, 2 and 5, the values in Table 5 have been referenced to 2005.0. Here we adopt the secular changes (Sect. 3) da/dt = 2.86 mm year^{-1} and

Table 5 Best fitting ellipsoid in the mean tide system, use of MDT and data coverage

Parameter	Year			MSL	MDT
	1998.5 (DNSC08)	1996.0 (CLS01)	2005.0		
Δa (m)		0.946 ± 0.001	0.972 ± 0.001	CLS01	–
		0.656 ± 0.001	0.682 ± 0.001	CLS01	ECCO-2
		-0.189 ± 0.001[a]	-0.163 ± 0.001[a]	CLS01	–
	0.949 ± 0.001			DNSC08	–
	0.664 ± 0.001			DNSC08	ECCO-2
Δb (m)		-0.631 ± 0.001	-0.603 ± 0.001	CLS01	–
		-0.058 ± 0.001	-0.030 ± 0.001	CLS01	ECCO-2
		6.659 ± 0.002[a]	6.687 ± 0.002[a]	CLS01	–
	-0.594 ± 0.001			DNSC08	
	-0.028 ± 0.001			DNSC08	ECCO-2
$W_0 = U_0$ ($\mathrm{m^2\,s^{-2}}$)		62636854.52 ± 0.01	62636854.26 ± 0.01	CLS01	–
		62636854.53 ± 0.01	62636854.27 ± 0.01	CLS01	ECCO-2
		62636838.05 ± 0.02[a]	62636837.79 ± 0.02[a]	CLS01	–
	62636854.37 ± 0.02		62636854.18 ± 0.01	DNSC08	–
	62636854.38 ± 0.02		62636854.19 ± 0.01	DNSC08	ECCO-2

[a] Ocean data only

db/dt = 3.11 mm year^{-1}. For CLS01 without ECCO-2, there is relatively poor agreement between the tabulated values ($62636854.01\,\mathrm{m^2\,s^{-2}}$ and $62636854.26\,\mathrm{m^2\,s^{-2}}$) on using the largest latitudinal extents but for DNSC08 ($62636854.24\,\mathrm{m^2\,s^{-2}}$ and $62636854.18\,\mathrm{m^2\,s^{-2}}$) the agreement is much better. With MDT, the CLS01-based values have not improved significantly ($62636854.05\,\mathrm{m^2\,s^{-2}}$ and $62636854.27\,\mathrm{m^2\,s^{-2}}$) while the DNSC08 values have not changed significantly from the values without MDT. On using the DNSC08, T/P and J1 values with MDT and the largest latitudinal extent from Tables 2, 3, 4 and 5, the agreement is excellent with mean value $62636854.21 \pm 0.04\,\mathrm{m^2\,s^{-2}}$ where the standard deviation was derived using the different estimates. It is noted that, even in this best case, the formal errors in the tables are less than the standard deviation of the mean. However, the formal errors are merely dependent on the data used and only reflect the internal accuracy of the solutions. For example, the errors budget of the EGM2008 geoid (Pavlis et al. 2008) over land and coastal areas will increase the standard errors of Table 5.

Burša et al. (2007a) suggested that the use of $\pm 0.5\mathrm{m^2\,s^{-2}}$ should be a safe estimate for the standard deviation. This value includes a possible 2–3 cm systematic altimeter calibration error that affects the solutions. Given that the T/P absolute bias is 0 ± 15mm (Haines et al. 2010), a standard deviation of $0.2\,\mathrm{m^2\,s^{-2}}$ is assumed appropriate giving $W_0 = 62636854.2 \pm 0.20\,\mathrm{m^2\,s^{-2}}$ as our estimation of W_0 for the global geoid at epoch 2005.0. Finally, in the mean tidal reference system, the values for Δa and Δb give $a = 6378136.964$m and $b = 6356751.573$ m (DNSC08 with ECCO-2), with flattening, $f = 1/298.247386$ at epoch 1998.5.

3 dW_0/dt: Methodology

If the geoid height or mass distribution changes, the geopotential value will also change according to

$$\Delta W_0(\phi, \lambda, r) = \left.\frac{\partial W_0}{\partial r}\right|_{P_0} \Delta r + \left.\frac{\partial W_0}{\partial C_{nm}}\right|_{P_0} \Delta C_{nm} + \left.\frac{\partial W_0}{\partial S_{nm}}\right|_{P_0} \Delta S_{nm} \quad (14)$$

The first term in the right hand side of Eq. (14) is related to the change in the geoid height and can be written as

$$\left.\frac{\partial W_0}{\partial r}\right|_{P_0} = \left[-\frac{\mathrm{GM}}{a_{\mathrm{E}}^2}\sum_{n=0}^{\infty}(n+1)\left(\frac{a_{\mathrm{E}}}{r}\right)^{n+2}\sum_{m=0}^{n}(C_{nm}\cos m\lambda + S_{nm}\sin m\lambda)P_{nm}(\sin\phi)\right] + \omega^2 r\cos^2\phi \quad (15)$$

while the other terms are due to the change in harmonic coefficients, namely

$$\frac{\partial W_0}{\partial C_{nm}} = \frac{\mathrm{GM}}{a_{\mathrm{E}}}\left(\frac{a_{\mathrm{E}}}{r}\right)^{n+1} P_{nm}(\sin\phi)\cos m\lambda \quad (16)$$

and

$$\frac{\partial W_0}{\partial S_{nm}} = \frac{\mathrm{GM}}{a_{\mathrm{E}}}\left(\frac{a_{\mathrm{E}}}{r}\right)^{n+1} P_{nm}(\sin\phi)\sin m\lambda \quad (17)$$

In Eq. (14), ΔC_{nm} and ΔS_{nm} are obtained from GRACE and SLR, while Δr is obtained from altimetry where we can take $\Delta r = \Delta N$, N being the geoid height.

3.1 GRACE data

We have used 78 monthly GRACE gravity fields from the CSR Release 4 over the period 2002.4–2009.0 (ftp://podaac.jpl.nasa.gov/pub/grace/data/L2/csr/RL04). The background atmospheric and ocean models were restored as the processing was performed over the oceans. We applied spatial averaging (Wahr et al. 1998) with a 400-km Gaussian averaging kernel (Jekeli 1981) and destriping (Swenson and Wahr 2006) to harmonics of degree $n > 8$. The C_{20} coefficients from GRACE were replaced by those from SLR. For temporal variations in the Earth's gravity field due to mass redistribution, we take into account variability in the degree one terms representing the Earth's geocentre. Seasonal signatures and trends in the degree one harmonics can have an effect on ocean mass trends of a few tenths of mm year^{-1} (Swenson et al. 2008). Such trends need consideration as $\mathrm{d}W_0/\mathrm{d}t$ will reflect any temporal signatures in the MSL figure. Degree one harmonics were taken from Swenson et al. (2008) as inferred from GRACE and an ocean model. There are alternative degree one time series such as from satellite laser ranging but Swenson et al. (2008) show excellent agreement between the GRACE-based harmonics and those from satellite tracking.

The gravity field model GGM03C (Tapley et al. 2007) was adopted as the static field. This field was removed from each of the GRACE monthly fields up to degree and order 60 with time variations in C_{nm} and S_{nm} estimated relative to 2006.0. Contemporaneous mean sea surface heights from the Jason-1 mission, were used to determine variations in N_r. However, as GRACE data are supplied on a monthly frequency and Jason-1 on 10-day cycles, we merged Jason cycles to match the GRACE fields as closely as possible. Further, several Jason-1 cycles were discarded as the GRACE fields did not cover the entire time span of Jason-1. It is not appropriate to use the monthly ECCO-2 fields as there is a component due to sea-level change (e.g., the steric effect) that would also be removed from the Jason-1 altimetric heights. Accordingly, MDT was neglected and $\Delta N_r = \Delta h_r$.

3.2 $\mathrm{d}W_0/\mathrm{d}t$: Sea level and GRACE

Time variations of the harmonic coefficients and the geoid height were used in Eq. (14) to compute the monthly variations of the gravity potential at each grid point of the MSL. The variations then were averaged globally using the equal area weighting function to obtain monthly variations of the geopotential (Fig. 3). Solution for a bias, trend and annual and semi-annual signals yielded $\mathrm{d}W_0/\mathrm{d}t = -2.59 \times 10^{-2} \pm 0.19 \times 10^{-2}\ \mathrm{m^2\,s^{-2}\,year^{-1}}$ from the combined effects of sea level change and gravity field variations. To find the contribution of sea level change, we set $\Delta C_{lm} = \Delta S_{lm} = 0$in Eq. (14). The results almost replicated Fig. 3 giving $\mathrm{d}W_0/\mathrm{d}t = -2.60 \times 10^{-2} \pm 0.17 \times 10^{-2}\ \mathrm{m^2\,s^{-2}\,year^{-1}}$. Similarly, setting $\Delta r = 0$ in Eq. (14) yielded the effect of the harmonic variations (Fig. 4) and produced a negligible positive trend of $\mathrm{d}W_0/\mathrm{d}t = 0.99 \times 10^{-5} \pm 1.00 \times 10^{-4}\ \mathrm{m^2\,s^{-2}\,year^{-1}}$. This signal was further investigated to derive the contributions $\mathrm{d}W_0/\mathrm{d}t = 2.1 \times 10^{-4} \pm 0.6 \times 10^{-4}\ \mathrm{m^2\,s^{-2}\,year^{-1}}$ from ΔC_{20} (Fig. 5) and the remaining harmonics (excluding degree 1) $\mathrm{d}W_0/\mathrm{d}t = -1.6 \times 10^{-4} \pm 0.6 \times 10^{-4}\ \mathrm{m^2\,s^{-2}\,year^{-1}}$ (Fig. 6). The effect of the degree one harmonics is insignificant.

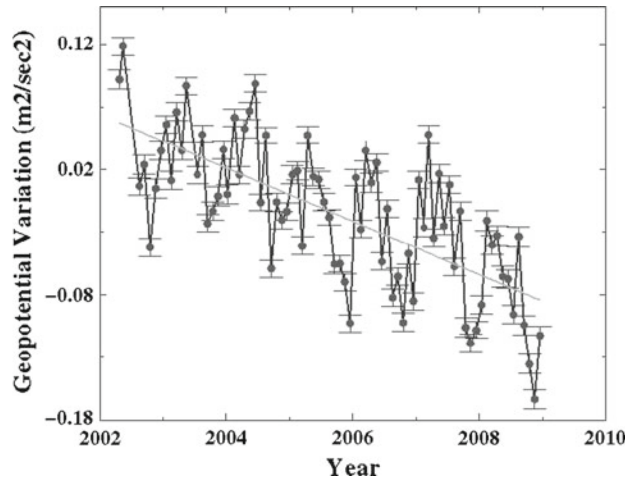

Fig. 3 Monthly geopotential variations from GRACE and Jason-1. Trend $\mathrm{d}W_0/\mathrm{d}t = -2.591 \times 10^{-2} \pm 0.195 \times 10^{-2}\ \mathrm{m^2\,s^{-2}\,year^{-1}}$

3.3 $\mathrm{d}W_0/\mathrm{d}t$ from TOPEX and Jason-1

The previous analysis established that the contribution of gravity field variations to $\mathrm{d}W_0/\mathrm{d}t$ is negligible. Therefore, it was decided to ignore this contribution and utilize a longer time series of sea level measurements to estimate $\mathrm{d}W_0/\mathrm{d}t$. Accordingly, sea level heights from TOPEX/Poseidon and Jason-1 missions between 1992.9 and 2009.0 (see Sect. 2.1.2) were used. The gravity potentials were estimated per cycle at each grid point of the sea-surface height using EGM2008 to degree and order 360 in the mean tide system. The resulting potentials values were averaged globally to compute the geopotential value for each cycle from TOPEX and Jason-1 (Fig. 7). Solving for a bias, trend and annual and semi-annual signals yielded $\mathrm{d}W_0/\mathrm{d}t = -2.70 \times 10^{-2} \pm 0.03 \times 10^{-2}\ \mathrm{m^2\,s^{-2}\,year^{-1}}$. This is our best estimate of $\mathrm{d}W_0/\mathrm{d}t$.

We note that our 1992–2009 value obtained with the IB correction applied is larger than the 1992–2003 value $\mathrm{d}W_0/\mathrm{d}t = -3.0\times10^{-4} \pm 3.6\times10^{-4}\ \mathrm{m^2\,s^{-2}\,year^{-1}}$ given by

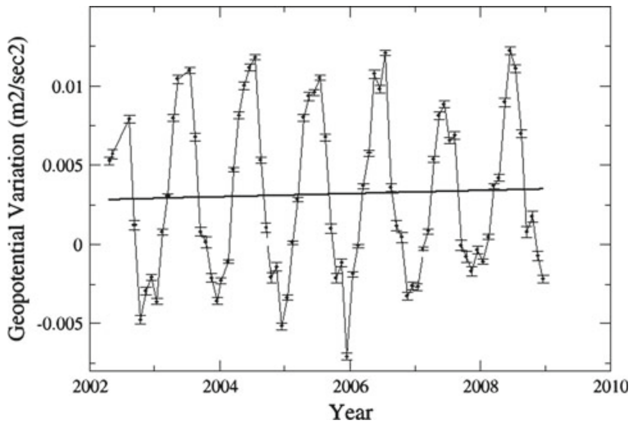

Fig. 4 Monthly geopotential variations from GRACE. Trend $\mathrm{d}W_0/\mathrm{d}t = 0.99 \times 10^{-5} \pm 1.00 \times 10^{-4}\ \mathrm{m}^2\,\mathrm{s}^{-2}\,\mathrm{year}^{-1}$

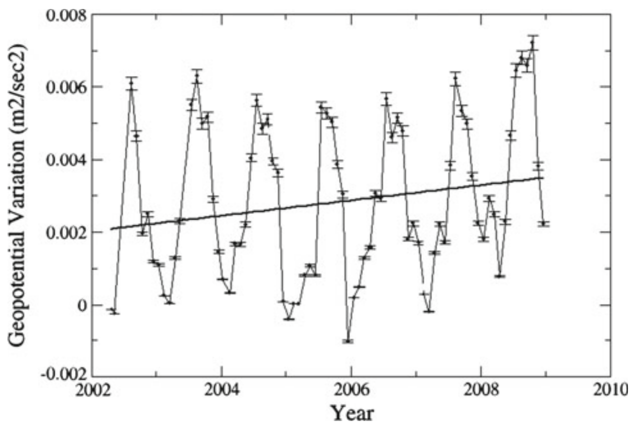

Fig. 5 The contribution of ΔC_{20} to the geopotential variations. Trend $\mathrm{d}W_0/\mathrm{d}t = 2.1 \times 10^{-4} \pm 0.6 \times 10^{-4}\ \mathrm{m}^2\,\mathrm{s}^{-2}\,\mathrm{year}^{-1}$

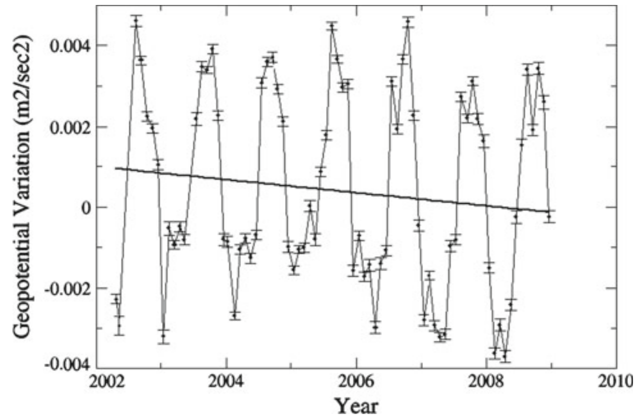

Fig. 6 The contribution of the harmonic coefficient variations excluding the first degree coefficients and ΔC_{20} to $\mathrm{d}W_0/\mathrm{d}t$. Trend $\mathrm{d}W_0/\mathrm{d}t = -1.6 \times 10^{-4} \pm 0.6 \times 10^{-4}\ \mathrm{m}^2\,\mathrm{s}^{-2}\,\mathrm{year}^{-1}$

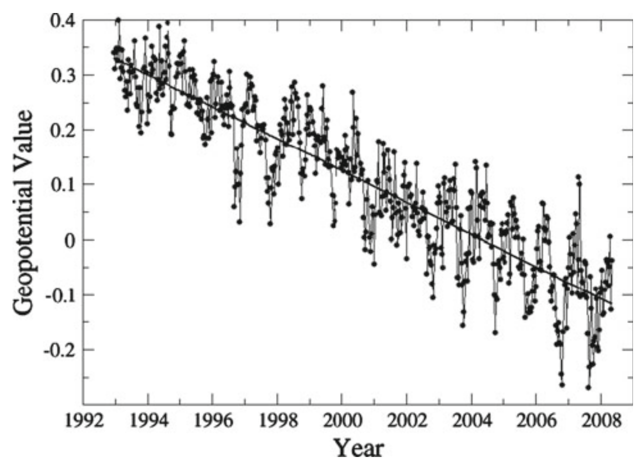

Fig. 7 Change in W_0 per cycle from TOPEX and Jason-1 (1992.9–2009.0). Trend $\mathrm{d}W_0/\mathrm{d}t = -2.70\times10^{-2}\pm0.0.03\times10^{-2}\ \mathrm{m}^2\,\mathrm{s}^{-2}\,\mathrm{year}^{-1}$

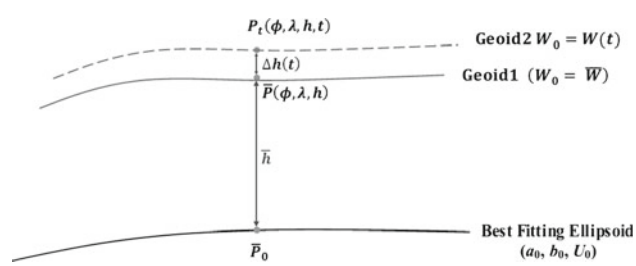

Fig. 8 Best fitting ellipsoid to the geoid

Burša et al., (2007) but in agreement with $-2.50\times10^{-2}\ \mathrm{m}^2\,\mathrm{s}^{-2}\,\mathrm{year}^{-1}$ for 1993–2001 estimated by Sanchez (2007). The differences with Burša et al., (2007) may be due in part to the altimetry processing. In our work, we used the first 364 cycles of TOPEX after which T/P was maneuvered to a new orbit and replaced in the original orbit by Jason-1. TOPEX cycles after 365 were not used. Also we used the sea-state bias correction for TOPEX_A and TOPEX_B altimeters as given by (Chambers et al. 2003). Similarly, we applied the known drift in one channel of the TOPEX microwave radiometer (TMR) (Keihm et al. 1998, 2000) for the wet tropospheric correction. Our derived global sea-level change (see Sect. 3.4) of ≈ 2.9 mm year^{-1} is also in agreement with (Cazenave and Nerem 2004) and (Leuliette et al. 2004) that give of sea level rise of 3.1 ± 0.7 mm year^{-1} between 1993 and 2003.

3.4 $\mathrm{d}W_0/\mathrm{d}t$ from the normal gravity field

Similar to Sect. 2.2, $\mathrm{d}W_0/\mathrm{d}t$ can be estimated indirectly within the normal gravity field by calculating secular changes in the semi-major axis, a, and semi-minor axis, b, of the best fitting ellipsoid to the geoid. In Fig. 8, $E_0(a_0, b_0, U_0)$ is the best fitting ellipsoid to the geoid1 and (cf. Eq. 7) satisfies

$$\min \int_{S_0} \left(\frac{T_{\overline{P}(t)}}{\gamma(\overline{P}_0)} \right)^2 \mathrm{d}S \tag{18}$$

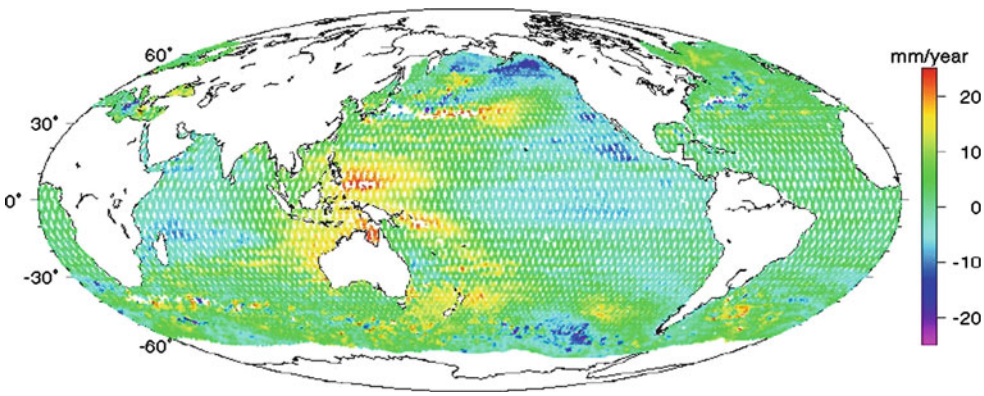

Fig. 9 Sea level trends from the T/P mission, cycles 9–364

where $T_{\overline{P}(t)}$ is the disturbing potential at $\overline{P}$ on the geoid at time t. If geoid1 moves to geoid2 at time t the position of the point $\bar{P}(\phi, \lambda, h)$ will change by radial distance Δh to $P_t(\phi, \lambda, h, t)$. $E_0(a_0, b_0, U_0)$ satisfies Eq. (18) for geoid1 but not for the shifted geoid2. Accordingly, the ellipsoid has to be modified to best fit the new surface. This involves solving Eq. 18 for changes to a_0 and b_0. Using

$$T_{P_t} = W_{P_t} - U_{P_t} \tag{19}$$

we linearize in time to give

$$T_{P_t} = W_{\bar{P}} + \left.\frac{\partial W}{\partial h}\right|_{\bar{P}} \frac{\mathrm{d}h}{\mathrm{d}t} - U_{\bar{P}_0} - \left.\frac{\partial U}{\partial a}\right|_{\bar{P}_0} \frac{\mathrm{d}a}{\mathrm{d}t} - \left.\frac{\partial U}{\partial b}\right|_{\bar{P}_0} \frac{\mathrm{d}b}{\mathrm{d}t} \tag{20}$$

As $\left.\frac{\partial W}{\partial h}\right|_{\bar{P}} \approx -\gamma(a_0, b_0, \overline{P})$, the normal gravity acceleration on the surface of the best fitting ellipsoid, and $W_{\bar{P}} = U_{\bar{P}_0}$ by definition of the best fitting ellipsoid, then

$$\hat{T} = W_{\bar{P}} + \left.\frac{\partial W}{\partial h}\right|_{\bar{P}} \frac{\mathrm{d}h}{\mathrm{d}t} - U_{\bar{P}_0} = -\gamma(a_0, b_0, \overline{P})\frac{\mathrm{d}h}{\mathrm{d}t} \tag{21}$$

As in Eq. (7), we can take $\gamma(a_0, b_0, \overline{P}) \approx \gamma(a_r, b_r, \overline{P}) \equiv \overline{\gamma}$ and hence, using Eq. (20)and Eq.(21), approximate Eq. (18) with

$$\min \sum_{\text{Earth}} \left(\Delta h + \frac{1}{\overline{\gamma}} \left.\frac{\partial U}{\partial a}\right|_{\bar{P}_0} \Delta a + \frac{1}{\overline{\gamma}} \left.\frac{\partial U}{\partial b}\right|_{\bar{P}_0} \Delta b \right)^2 \times \cos\phi \Delta\phi \Delta\lambda \tag{22}$$

where the summation is over lat/long bins of size $\Delta\phi$ and $\Delta\lambda$. In Eq. (22), Δa and Δb are the changes in a and b associated with the change Δh in the geoid height.

In this approach, a complete reference geoid surface and its best fitting ellipsoid need to be known initially. These were taken as a $1° \times 1°$ geoid constructed from DNSC08 and ECCO-2 over the ocean and from the EGM2008 geoid over the remaining areas. We also adopted the best fitting ellipsoid defined by $a = 6378136.964$m and $b = 6356751.573$ m of Sect. 2.2. Furthermore, in Eq. (22), Δh needs to be known at each grid point. For this, we use time series from TOPEX data (cycles 9–364) at the standard latitudinal points as in Sect. 2.1.2. At each standard point we solved for the trend and, as previously, for the aliased tidal constituents O1, K1, N2, M2, S2, K2 and SA. This produced sea level changes which are presented in Fig. 9. Averaging these globally produced a mean global sea level rise of $\approx$2.9 mm year^{-1}

The trends at the standard latitudinal point were interpolated onto a $1° \times 1°$ grid. Measurements from radar altimetry are provided only over the ocean for latitudes between 66°N and 66°S. Here, we proposed three cases based on the handling of areas in Fig. 9 where geoid rates are not available. In Case 1, the trend over these data free zones was taken as zero, while the global mean of 2.9 mm year^{-1} was considered in Case 2. Case 3 considers oceanic rates only. Results in Table 6 indicate that $\mathrm{d}W_0/\mathrm{d}t$ from Case 2 is the best estimate in terms of consistency with our previous results, while Case 3 gave unrealistic results showing the necessity of a global dataset when using the normal gravity field. We note that the Case 2 value can be obtained in an iterative refinement procedure starting with say a trend of zero mm year^{-1} over data free zones and replacing successively with the refined global trend. Our Case 2 value for $\mathrm{d}W_0/\mathrm{d}t$ agrees within the quoted errors with the result in Sect. 3.3.

4 Critique, discussion and conclusions

The objective of the study was to quantify W_0 that best represents MSL at a specified epoch. Although for global vertical datum unification, the reference level may refer to a value of W_0 based on some convention, there is merit in adopting a value that coincides with MSL at a given epoch.

The study demonstrated that recovery of W_0 is almost independent of the choice of GGM and, in particular, the high degree harmonics (i.e., $n > 120$). Furthermore, the dependency of W_0 on oceanic data coverage is merely due to MDT. Conversely, MDT is the main factor that influences estima-

Table 6 The secular trends in a, b and W_0 from TOPEX mission in the normal gravity field from three different cases according to the trend applied for data free zones

Parameter	$\dot{a}$ (mm year^{-1})	$\dot{b}$ (mm year^{-1})	$\mathrm{d}U_0/\mathrm{d}t = \mathrm{d}W_0/\mathrm{d}t$ (m^2 s^{-2} year^{-1})	Data free zone trend (mm year^{-1})
Case 1	2.38 ± 0.01	0.94 ± 0.02	-0.0187 ± 0.001	0.0
Case 2	2.86 ± 0.01	3.11 ± 0.02	-0.0288 ± 0.001	2.9
Case 3	-1184.32 ± 0.13	4955.92 ± 0.27	-8.505	No data

tion of W_0. The choice of MDT model is somewhat arbitrary and different values of W_0 may result as a consequence of differences in the geopotential surface that corresponds to the zero level, i.e., MDT = 0. It is, thus, important to identify the value of W_0 with the MDT model used in the estimation procedure.

W_0 has been recovered using various GGMs and MSL models and the normal gravity field. The preferred value utilizes DNSC08 as that model incorporates an extensive altimetric data base along with recent enhancements to the altimetric corrections. On adjusting for MDT with ECCO-2, there is consistency ($W_0 = 62636854.21 \pm 0.04$ m^2 s^{-2} at epoch 2005.0) between solutions using DNSC08, T/P, J1 and the normal gravity field. The scatter in the mean value equates to about 3σ where sigma is the formal standard deviation in the tables. This level of agreement establishes that DNSC08, T/P and J1 mean sea levels correspond to the same altimetric datum. The error associated with W_0 is, however, adjusted to reflect a possible systematic 15 mm altimeter calibration error in the T/P altimetric range data and a non-zero MDT datum at epoch 2005.0. Accordingly, a 0.2 m^2 s^{-2} standard deviation is considered appropriate. Significantly, our W_0 differs by 1.8 m^2 s^{-2} from 62636856.0 ± 0.5 m^2 s^{-2} (Burša et al. 2007a) incorporated within the IAU 2009 system of astronomical constants.

For a critical review of published values, it is necessary to refer to estimation of W_0 without adjustment for MDT and, given the temporal change in mean sea-level height, to adopt a consistent reference epoch. In Table 7, we summarise published results for W_0 for epoch 2005.0 and for latitudinal ranges that are a close fit to the tabulated extent. The Sanchez (2007, 2009) results have been adjusted to epoch 2005.0 from the 2000.0 epoch used in those studies. In terms of methodology Sanchez (2007) used method (i) of Sect. 2 without correction for MDT while Sanchez (2009) attempted to remove the effect of MDT by minimizing the dynamic topography with respect to W_0 over the ocean surface. The resultant expression introduces an additional factor of $1/\gamma_P^2$ into the areal averaging procedure over the latitudinal extent of the MSL grid. However, the results still exhibits a variation depending on the latitudinal extent of the ocean surface used in the computation. All values in the table show a similar increase as the latitudinal extent increases from 60°N/60°S to 82°N/80°S.

As expected, given identical computational strategies, our value for CLS01 and EGM96 at epoch 2005.0 is in total agreement with Sanchez (2007). Other values in Table 7 use a number of similar gravity field models but different MSL models including CLS01, DNSC08, KMS04 (Andersen et al. 2004) and GSFC00.1 (Koblinsky et al. 1999). The 0.2 m^2 s^{-2} difference (equivalent to 2 cm in height) between CLS01 and KMS04 and DNSC08 is likely to be caused by averaging the ocean variability over different time periods as well as enhancements (and additional data) in KMS04 and DNSC08 in particular.

There is a disparity in Table 7 between the results of this study and Sanchez (2007, 2009) with those from (Burša et al. 2007a. It is noted that in a later study (Burša et al. 2007b), $W_0 = 62636854.784$ m^2 s^{-2} (62636854.586 m^2 s^{-2}) is presented from ice-free T/P (J1) altimetry for 1993–2005 (2003–2005). The extent of the ice-free area is dependent on the year and differs from our usage of an ice-free area where data were available over 75% of the repeat cycles. However, the main difference is the ellipsoidal height correction (0.13 m for TOPEX/Poseidon) applied by (Burša et al. 2007b) to correct T/P to the Jason-1 mean sea surface. This value is equivalent to the early J1 bias (Haines et al. 2003). However, as T/P is effectively the unbiased MSL (Haines et al. 2010), the correction should be applied to J1 which would yield a W_0 value that is once more close to the IAU value. We are thus unable to explain the 1.8m^2 s^{-2} between our value and Burša et al. (2007a).

The variation with latitude disappears with direct use of the ECCO-2 MDT model in our study (see Tables 1, 2). We conclude that MDT is the cause of the latitudinal variation of Table 7. By utilizing a MDT model, there is convergence of values over 60°S–60°N and 70°S – 70°N for a given mean sea surface model. Our value $W_0 = 62636854.2 \pm 0.2$ m^2 s^{-2} at epoch 2005.0 has, therefore, been derived from a robust representation of the gravitational level surface that equates to MSL after correction for MDT. The value is consistent with known biases in the altimetric data sets.

Consideration of the DNSC08 numerical values for 60°N–60°S in Tables 1 and 2 shows that without MDT W_0 is too low or equivalently MSL too high. Thus, from Eq. (3) MDT is on average positive in sign. For latitude band 70°N–70°S, The values of Tables 1 and 2 agree and MDT has near zero effect. However, when extended to 82°S–80°N, the

Table 7 Published values of W_0 ($m^2 s^{-2}$) from different methodologies, GGM and MSL models. MDT not considered

Reference	MSS	GGM	W_0 60N–60S	W_0 82N–80S
Burša et al. (2007a)	T/P	EGM96	62636855.81	
Burša et al. (2007b)	T/P	EGM96	4.60[a]	
Sanchez (2007)	CLS01	EGM96	3.23	4.48
	CLS01	EIGEN-CG03C	3.22	4.48
	KMS04	EIGEN-CG03C	3.11	4.33
	GSFC00.1	EIGEN-CG03C	3.45	4.80
Sanchez (2009)	CLS01	EGM96	3.03	4.26
	CLS01	EIGEN-GL04S	2.98	4.25
This study	CLS01	EGM96	3.24	4.25
	CLS01	EIGEN-GL04C	3.20	4.23
	CLS01	EGM2008	3.19	4.22
	DNSC08	EGM2008	3.43	4.43
	T/P	EGM2008	3.31	
	J1	EGM2008	3.27	
	DNSC08	Normal field		4.18

All values at epoch 2005.0 with latitudinal range a best match to data
[a] Ice free area

DNSC08 W_0 is high compared with our recommended value with the inference that MDT has a negative average over this range. Such inferences are consistent with MDT models such as DNSC08 (Andersen and Knudsen 2009). Thus, over 70°N–70∘S, the large negative MDT over the Antarctic circumpolar current (ACC) balances the positive MDT over 60°N/60°S. For 82°S/80°N the complete ACC is included with only the northern Arctic Ocean excluded. It is significant to note that if the MDT over 82°S/80°N is minimized with respect to W_0 as in Sanchez (2009), the resultant value is $62636854.21 \pm 0.03\ m^2 s^{-2}$. That our recommended value agrees almost exactly with this value confirms that, it is feasible to use either the Sanchez (2009) approach over the full extent of a MSL model or the latitude band 70°N–70°S without MDT to derive an unbiased value for W_0.

This study also shows that estimation of the secular trend of W_0 is mainly influenced by sea level change, while variations of Earth gravity field, including the degree 1 harmonics, play a negligible part. Again it is possible to determine dW_0/dt within the normal gravity field on the condition that the geoid height change is available over the entire Earth. Our best estimate of dW_0/dt from the global approach is based on TOPEX and Jason-1 data between 1992.9 and 2009.0 namely $dW_0/dt = -2.70 \pm 0.05 \times 10^{-2}\ m^2 s^{-2}\ year^{-1}$ which equates to a global sea-level rise of 2.9 mm year^{-1}. This value is in close agreement with $-2.50 \times 10^{-2}\ m^2 s^{-2}$ year^{-1} for 1993–2001 estimated by Sanchez (2007) with difference due to increased sea-level rise over the last few years (Beckley et al. 2007).

From a detailed analysis and examination of altimetric sea surfaces, we have established the value $W_0 = 62636854.2 \pm 0.2\ m^2 s^{-2}$ at epoch 2005.0 with secular variation $dW_0/dt = -2.70 \pm 0.05 \times 10^{-2}\ m^2 s^{-2}\ year^{-1}$ as a better definition of the geoid in the sense of Gauss–Listing than the IAU 2009 value. As a consequence, the derived value and its rate can be used for unification of vertical datums with respect to MSL in a world height system. Conversion of geopotential numbers to height is then a process of realization (Sanchez 2007). It is of course necessary to continue to monitor dW_0/dt and to note any departures from linearity in the future. In addition, it is important to incorporate later altimetric missions such as Jason-2 into the MSL models and to note any enhancements in altimetric processing particularly those that affect the altimeter biases and consequently the altimetric datums of the missions.

Acknowledgments The authors wish to thank Prof. Pavel Novak for comments and discussions that have greatly improved the content and clarity of this paper.

References

Andersen OB, Knudsen P (2009) DNSC08 mean sea surface and mean dynamic topography models. J Geophys Res Oceans 114:C11001. doi:10.1029/2008JC005179

Andersen OB, Vest AL, Knudsen P (2004) KMS04 mean sea surface model and inter-annual sea level variability. In: Poster presented at EGU General Assembly 2005, Vienna, Austria, 24–29, April 2005

Ardalan A, Grafarend E, Kakkuri J (2002) National height datum, the Gauss–Listing geoid level value W_0 and its time variation, Baltic Sea Level project: epochs 1990.8, 1993.8, 1997.4). J Geod 76:1–28

Beckley BD, Lemoine FG, Luthcke SB, Ray RD, Zelensky NP (2007) A reassessment of global and regional mean sea level trends from TOPEX and Jason-1 altimetry based on revised reference frame and orbits. Geophys Res Lett 34:L14608. doi:10.1029/2007GL030002

Burša M, Kenyon S, Kouba J, Müller A, Radej K, Vatrt V, Vojtíšková M, Vítek V (1999a) Long-term stability of geoidal geopotential FromTopex/Poseidon satellite altimetry 1993–1999. Earth Moon Planets 84:163–176

Burša M, Kenyon S, Kouba J, Radej K, Vatrt V, Vojtíšková M,Šimek J (2001) World height system specified by geopotential at tide gauge stations, vol 124. In: IAG Symposia. Springer, Berlin, pp 291–296

Burša M, Kenyon S, Kouba J, Šíma Z, Vatrt V, Vítek V, Vojtíšková M (2007a) The geopotential value W0 for specifying the relativistic atomic time scale and a global vertical reference system. J Geod 81:103–110

Burša M, Kenyon S, Kouba J, Šíma Z, Vatrt V, Vojtíšková M (2004) A global vertical reference frame based on four regional vertical datums. Studia Geophysica et Geodaetica 48:493–502

Burša M, Kouba J, Kumar M, Müller A, Radej K, True SA, Vatrt V, Vojtíšková M (1999b) Geoidal geopotential and world height system. Studia Geophysica et Geodaetica 43:327–337

Bursa M, Ouba JK, Adej KR, True SA, Atrt VV, Vjtiskova MV (1998) Monitoring geoidal potential on the basis of TOPEX/POSEIDON altimeter data. In: IAG Scientific Assembly, Rio di Janeiro. Springer, Berlin, pp 352–358

Burša M, Radej K, Šima Z, True SA, Vatrt V (1997) Determination of the geopotential scale factor from TOPEX/POSEIDON satellite altimetry. Studia Geophysica et Geodaetica 41:203–216

Burša M, Šíma Z, Kenyon S, Kouba J, Vatrt V, Vojtíšková M (2007b) Twelve years of developments: geoidal geopotential w0 for the establishment of a world height system—present state and future. In: Proceedings of the 1st international symposium of the international gravity field service, Harita Genel Komutanligi, Istanbul, pp 121–123

Cazenave A, Nerem RS (2004) Present-day sea level change: observations and causes. Rev. Geophys 42:RG3001. doi:3010.1029/2003RG000139

Chambers DP (2006) Observing seasonal steric sea level variations with GRACE and satellite altimetry. J Geophys Res C Oceans 111:C03010

Chambers DP, Hayes SA, Ries JC, Urban TJ (2003) New TOPEX sea state bias models and their effect on global mean sea level. J Geophys Res 108:3305–3311

Chen JL, Wilson CR, Tapley BD, Famiglietti JS, Rodell M (2005) Seasonal global mean sea level change from satellite altimeter, GRACE, and geophysical models. J Geod 79:532–539

Cheng M, Tapley BD (2004) Variations in the Earth's oblateness during the past 28 years. J Geophys Res Solid Earth 109:B09402

Dorandeu J, Le Traon PY (1999) Effects of global mean atmospheric pressure variations on mean sea level changes from TOPEX/Poseidon. J Atmos Oceanic Technol 16:1279–1283

Förste C, Fletcher F, Schmidt R, Meyer U, Stubenvoll R, Barthelmes F, König R, Neumayer KH, Rothacher M, Reigber C (2005) A new high resolution global gravity field model derived from combination of GRACE and CHAMP mission and altimetry/gravimetry surface gravity data. In: European Geosciences Union General Assembly, Vienna, Austria (2005)

Förste C, Schmidt R, Stubenvoll R, Flechtner F, Meyer U, König R, Neumayer H, Biancale R, Lemoine JM, Bruinsma S, Loyer S, Barthelmes F, Esselborn S (2008) The GeoForschungsZentrum Potsdam/Groupe de Recherche de Geodesie Spatiale satellite-only and combined gravity field models: EIGEN-GL04S1 and EIGEN-GL04C. J Geod 82:331–346

Haines BJ, Desai SD, Born GH (2010) The Harvest experiment: calibration of the climate data record from TOPEX/Poseidon, Jason-1 and the Ocean Surface Topography Mission. Marine Geod 33:91–113

Haines BJ, Dong D, Born G, Gill S (2003) The Harvest experiment: monitoring Jason-1 and TOPEX/Poseidon from a California offshore platform. Marine Geod 26:239–259

Heiskanen WA, Moritz H (1967) Physical geodesy. W. H. Freeman, San Francisco

Hernandez F and Schaeffer P (2001) The CLS01 mean sea surface: a validation with the GSFC00.1 surface. Technical report CLS, Ramonville St Agne, 14pp

Hughes CW, Bingham RJ (2008) An Oceanographer's guide to GOCE and the geoid. Ocean Sci 4:15–29

Jekeli C (1981) Alternative method to smooth the Earth's gravity field. Department of Geodetic Science and Surveying, Ohio State University, Columbus

Keihm S, Zlotnicki V, Ruf C, Haines B (1998) TMR drift and scale error assessment. Report to TOPEX Project, Jet Propulsion Laboratory

Keihm SJ, Zlotnicki V, Ruf CS (2000) TOPEX microwave radiometer performance evaluation, 1992–1998. IEEE Trans Geosci Remote Sens 38:1379–1386

Koblinsky CJ, Ray RD, Beckeley BD, Wang Y-M, Tsaoussi L, Brenner A, Williamson R (1999) NASA ocean altimeter Pathfinder project report 1: Data processing handbook, NASA/TM-1998-208605

Lemoine FG, Kenyon SC, Factor JK, Trimmer RG, Pavlis NK, Chinn DS, Cox CM, Klosko SM, Luthcke SB, Torrence MH (1998) The Development of the Joint NASA GSFC and the National Imagery and Mapping Agency(NIMA) Geopotential Model EGM 96, NASA

Leuliette EW, Nerem RS, Mitchum GT (2004) Calibrationof TOPEX/Poseidon and Jason Altimeter Data to Construct a Continuous Record of Mean Sea Level Change. Marine Geod 27:79–94

Luzum B, Capitaine N, Fienga A, Folkner W, Fukushima T, Hilton J, Hohenkerk C, Krasinsky G, Petit G, Pitjeva E (2011) The IAU 2009 system of astronomical constants: the report of the IAU working group on numerical standards for Fundamental Astronomy. Cel Mech Dynam Astron 110(4):293

Menemenlis D, Campin JM, Heimbach P, Hill C, Lee T, Nguyen A, Schodlok M, Zhang H (2008) ECCO2: High resolution global ocean and sea ice data synthesis. Mercator Ocean Quart Newsl 31:13–21

Moore P, Zhang Q, Alothman A (2006) Recent results on modelling the spatial and temporal structure of the Earth's gravity field. Philos Trans Roy Soc A Math Phys Eng Sci 364(1009-1026):364, 1009–1026

Pavlis N, Kenyon S, Factor J, Holmes S (2008) Earth gravitational model 2008. In: SEG Technical Program Expanded Abstracts, pp 761–763

Rapp RH (1997) Use of potential coefficient models for geoid undulation determinations using a spherical harmonic representation of the height anomaly/geoid undulation difference. J Geod 71:282–289

Rio M-H, Schaeffer P, Lemoine J-M, Hernandez F (2005) Estimation of the ocean mean dynamic topography through the combination of altimetric data, in-situ measurements and GRACE geoid: from global to regional studies. In: Proceedings of the GOCINA international workshop

Sanchez L (2007) Definition and realisation of the SIRGAS vertical reference system within a globally unified height system. Dynamic Planet: Monitoring and Understanding a Dynamic Planet with Geodetic and Oceanographic Tools 130:638–645

Sanchez L (2009) Strategy to establish a global vertical reference system. In: Drewes H (ed) Geodetic reference frames, IAG symposia, vol 134. Springer, Berlin)

Schlax MG, Chelton DB (1996) Correction to "Aliased tidal errors in TOPEX/POSEIDON sea surface height data" by MG Schlax and DB Chelton. J Geophys Res Oceans 101:18451

Swenson S, Chambers D, Wahr J (2008) Estimating geocenter variations from a combination of GRACE and ocean model output. J Geophys Res Solid Earth 113:B08410

Swenson S, Wahr J (2006) Post-processing removal of correlated errors in GRACE data. Geophys Res Lett 33:L08402

Tapley B, Ries J, Bettadpur S, Chambers D, Cheng M, Condi F, Gunter B, Kang Z, Nagel P, Pastor R (2005) GGM02—an improved Earth gravity field model from GRACE. J Geod 79:467–478

Tapley B, Ries J, Bettadpur S, Chambers D, Cheng M, Condi F, Poole S (2007) The GGM03 mean Earth gravity model from GRACE. Eos Trans Am Geophys Union 88

Tapley BD, Bettadpur S, Chambers D, Cheng M, Choi K, Gunter B, Kang Z, Kim J, Nagel P and Ries J (2001) Gravity field determination from CHAMP using GPS tracking and accelerometer data: initial results. EOS Trans AGU 82:47

Tapley BD, Bettadpur S, Ries JC, Thompson PF, Watkins MM (2004) GRACE measurements of mass variability in the Earth system. Science 305(5683):503–505. doi:10.1126/science.1099192

Tapley BD, Watkins MM, Ries JC, Davis GW, Eanes RJ, Poole SR, Rim HJ, Schutz BE, Shum CK, R S Nerem Lerch, FJ Marshall, JA Klosko, SM Pavlis NK, Williamson RG (1996) The joint gravity model 3. J Geophys Res 101(28):029–028,049

Torge Wolfgang (1980) Geodesy, an introduction. De Gruyter, Berlin

Vaníček P, Krakiwsky EJ (1982) Geodesy: the concepts. Elsevier, Amsterdam

Wahr J, Molenaar M, Bryan F (1998) Time variability of the Earth's gravity field: hydrological and oceanic effects and their possible detection using GRACE. J Geophys Res Solid Earth 103:30205–30229

Zlotnicki V and Callahan P (2002) TOPEX and Jason Microwave Radiometer assessment against DMSP-SSM/I and TRMM/TMI. Paper read at Jason-1/TOPEX/Poseidon Science Working Team Meeting, 13–15 June, at Biarritz, France